

^{187}Re - ^{187}Os ISOTOPIC AND HIGHLY SIDEROPHILE ELEMENT SYSTEMATICS OF GROUP IVB IRONS. J. Honesto¹, W.F. McDonough¹, R.J. Walker¹, T.J. McCoy², and R.D. Ash¹. ¹Department of Geology, Univ. MD, College Park, MD 20742 (jhonesto@geol.umd.edu), ²Dept. of Mineral Sciences, National Museum of Natural History, Smithsonian Institution, Washington, DC, 20560-0119

Introduction: Study of the magmatic iron meteorite groups permits constraints to be placed on the chemical and isotopic composition of parent bodies, and the timing of, and crystal-liquid fractionation processes involved in the crystallization of asteroidal cores. Here we examine Re-Os isotopic and trace elemental systematics of group IVB irons. Compared to most irons, the irons comprising this group are enriched in some of the most refractory siderophile elements, yet highly-depleted in most volatile siderophile elements. These characteristics have been attributed to processes such as high temperature condensation of precursor materials [1] and oxidation in the parent body [2]. Most recently it has been suggested that both processes may be involved in the chemical complexity of the group [3]. Here, high precision isotopic and highly siderophile element (HSE) concentrations are used to further examine these possible origins, and the crystallization history of the group. In addition, we have begun to assess the possibility of relating certain ungrouped irons with major groups via multi-element, trace element modeling. In a companion abstract [4], the isotopic and trace element systematics of the ungrouped iron Tishomingo are compared with the IVB irons.

Analytical Methods: Chemical separation techniques used were similar to previous studies [5]. Blanks for Re, Pt, Os, Pd, Ru, and Ir averaged 7, 50, 2, 10, 10 and 1 pg, respectively. Osmium measurements were accomplished via negative thermal ionization mass spectrometry (*Sector 54*). The isotope dilution measurements of all other elements were done via static multi-collector ICP-MS (*Nu Plasma*) using faraday buckets. Fractionation was monitored and corrected via interspersal of samples with standards. Concentration data for these elements are $\pm 0.2\%$ or better.

Results: Concentrations of HSE are generally similar to those reported previously for IVB irons [e.g. 1-3](Table 1). Also, as has been previously noted, the range of concentrations of HSE is considerably less than for IIAB, IIIAB and IVA irons. There is only a factor of ~ 1.2 decrease in $^{187}\text{Re}/^{188}\text{Os}$ ratio from the least to most fractionated IVB irons.

A ^{187}Re - ^{187}Os isochron regression for the six IVB irons gives an age of 4610 ± 170 Ma (MSWD=1.9) and initial $^{187}\text{Os}/^{188}\text{Os} = 0.0951 \pm 0.0011$. This age is consistent with results of previous Re-Os studies [6,7]. Data for all six irons

are consistent with closed-system behavior subsequent to crystallization. Unlike for IIAB and IIIAB, there is insufficient spread in ^{190}Pt - ^{186}Os to enable generation of a meaningful isochron with current resolution.

Discussion: Chondrite normalized HSE patterns for the IVB irons form a continuous trend consistent with Re, Os, Ir, and Ru behaving as compatible elements during metal crystallization (Fig. 1). Lack of variation in Pt concentrations requires a solid metal-liquid metal bulk distribution coefficient of \sim unity. Palladium is the only element that behaves incompatibly among the group measured.

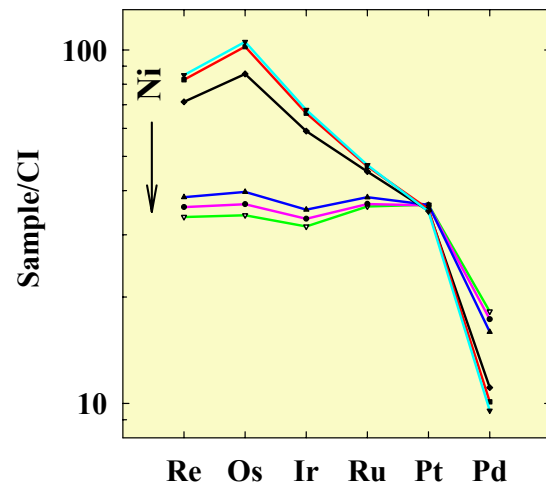


Fig. 1. CI chondrite normalized abundances of HSE for IVB irons. The HSE are plotted from left to right in order of increasing volatility.

With the exception of Re, there is a general drop in normalized abundance from the most refractory to least refractory HSE in the lowest Ni, least fractionated IVB irons (Fig. 1). Rhenium is significantly depleted relative to Os, despite very similar condensation temperatures. A plot of $\log[\text{Re}]$ vs. $\log[\text{Os}]$ for all IVB data gives a slope of 0.812 ± 0.087 (2σ). This slope can be used to estimate the relative solid metal-liquid metal partitioning behavior of Re vs. Os. A model for crystallization is presented in Fig. 2 using initial D_{Re} and D_{Os} values of 1.5 and 1.6 (appropriate for the slope and consistent with previous estimates for D_{Os}). For this model, a Re concentration of 2650 ng/g and a sub-chondritic $^{187}\text{Re}/^{188}\text{Os}$ of 0.34 are also assumed for the bulk

core. On the plot of Re vs. $^{187}\text{Re}/^{188}\text{Os}$ this model can account for all IVB compositions as primary solids, mixtures of solids and equilibrium liquids, or mixtures of early-formed solids and late-stage liquids. Although model parameters can be varied, these results invariably require a bulk core with very high concentrations of refractory HSE, relative to other asteroidal cores, and low Re/Os, relative to bulk chondrites. Formation of a core with such highly fractionated Re/Os is problematic, and quite distinct from IIAB, IIIAB and IVA groups [e.g. 5]. Because of similar solid metal-liquid metal D values, incomplete segregation of core could not result in such a large fractionation for Re from Os. Further, both elements have similar condensation temperatures and are difficult to oxidize, so they should be little fractionated from one another via either high temperature condensation, or oxidation processes. The hybrid model of [3] may not account for this peculiar chemical characteristic. We do note that on presumably smaller scales, similar, highly-fractionated Re/Os have been reported for CAIs [8] and bulk samples of the CK chondrite Karoonda [9].

References: [1] W.R. Kelly & J.W. Larimer (1977) *GCA* 41, 93-111 [2] Rasmussen *et al.* (1984) *GCA* 48, 805-813 [3] A. Campbell & M. Humayun. *GCA* in review [4] C.M. Corrigan *et al.* (2005) *LPSC* 36 [5] D.L.Cook *et al.* (2004) *GCA* 68, 1413-1431 [6] M.I. Smoliar *et al.* (1996) *Science* 271, 1099-1102 [7] J.J. Shen *et al.* (1996) *GCA* 60, 2887-2900 [8] H. Becker *et al.* (2001) *GCA* 65, 3379-3390 [9] R.J. Walker (2002) *GCA* 66, 4187-4201 [10] V.F. Buchwald (1975) *Handbook of Meteorites*.

This work was supported by NASA grants NNG04GG17G (WFM), NNG04GK52G (RJW), and NAG5-13464 (TJM).

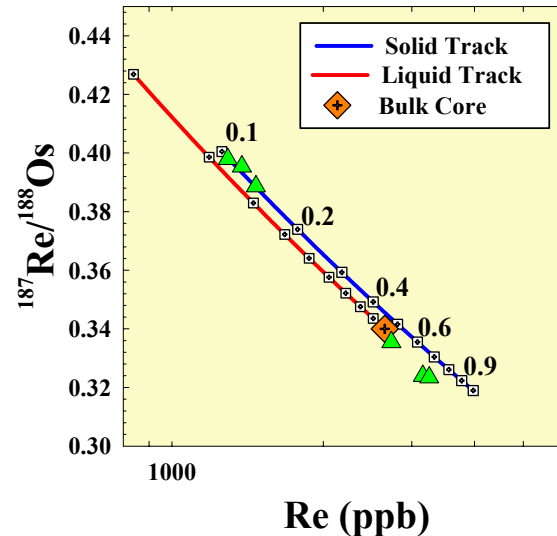


Fig. 2. Fractional crystallization model showing hypothetical liquid and solid tracks using parameters discussed in the text. Open squares correspond to the 10% fractions of liquid. All IVB data can be accounted for via fractional crystallization and solid-liquid mixing.

Table 1. Isotopic and HSE concentration data for IVB irons. Concentrations are in ng/g, except Ni, which is in wt %.

Sample	Ni*	Re	Os	Ir	Ru	Pt	Pd	$^{187}\text{Os}/^{188}\text{Os}$	$^{187}\text{Re}/^{188}\text{Os}$	Δ_{Os}
Warburton Range	18.02	1291	15630	14427	23448	31365	10252	0.12939	0.3979	1.5
Tawallah Valley	17.94	1378	16786	15178	23817	31242	9750.8	0.13011	0.3954	-1.0
Weaver Mountain	17.7**	1469	18203	16105	24894	31328	8974.1	0.12977	0.3886	-0.6
Hoba	16.33	2732	39206	26863	29436	30142	6244.1	0.13146	0.3354	0.0
Tlacotepec	15.60	3155	46891	30169	30459	30132	5691.6	0.13215	0.3239	-0.1
Cape of Good Hope	15.64	3249	48367	30848	30703	30026	5378.4	0.13465	0.3234	0.0

Δ_{Os} is the deviation of the $^{187}\text{Os}/^{188}\text{Os}$ of a sample datum from the IVB isochron in units of per mil. *[3], **[10]